Materials Transactions, JIM, Vol. 36, No. 2 (1995), pp. 188 to 197

Control of Structure and Formation of Amorphous and Nonequilibrium Crystalline Metals by Mechanical Milling (*Overview*)

K. Suzuki and K. Sumiyama

Institute for Materials Research, Tohoku University, Sendai 980-77, Japan

This review first describes a rod milling method developed by us. Using this method we utilize shear force more effectively than impact force for both comminution to nano-crystallites and amorphization, and minimize contamination problems. X-ray diffraction, transmission electron microscopy, neutron scattering and thermal analyses for milled powders elucidate the elemental processes of solid-state amorphization: 1) preferential mutation of octahedral units to tetrahedral units is indispensable for amorphization, where reconnection of tetrahedral units changes from vertex-sharing to face- and/or edge-sharing, 2) layered morphology produced in the initial stage of MA is highly energetic, leading to amorphization even by heating (thermally assisted solid state amorphization), 3) comminution to nano-crystallites is attributed to the glide of dislocations induced by shear force, and 4) in the ternary system, preferential alloying of binary constituents initially forms an intermetallic and such heterogeneous mixture gradually become a homogeneous amorphous phase. Mechanical milling is also powerful to produce nonequilibrium disordered crystalline alloys, whose equilibrium crystalline counter parts show immiscibility and/or very narrow primary solid solution ranges. Since milled powers is very fine and contains a large amount strain and defects, Al is removed from nonequilibrium crystalline and amorphous Al-transition metal alloys, leaving metastable transition metal powders.

(Received January 13, 1995)

Keywords: *mechanical milling, amorphous, nonequilibrium crystal, X-ray diffraction, neutron scattering, magnetic properties*

I. Introduction

Mechanical milling has attracted current attention as a means for forming nonequilibrium solid phases by controlling the valence electron state, atomic arrangement and nano-scale phase structure of materials through solid state reaction at ambient temperature[1)-3)]. Traditionally nonequilibrium solid phases such as amorphous alloys have been formed by means of the solidification from melts or the condensation from vapors[4)]. These conventional procedures are based on the rapid removal of the kinetic energy of atoms moving in the energized state of liquids or gases. In an alternative approach to the conventional procedures, atoms in the stable equilibrium crystalline state are mechanically excited, combined chemically if necessary, and frozen into the metastable state often having a topologically disordered atomic structure.

Such a solid state amorphizing reaction occurs by destroying the long-range periodic structure of crystalline solids under the irradiation with lights, electrons, neutrons or ions[4)5)]. In particular, current interests have been rather focused on the solid state amorphizing reaction using mechanical milling. Mechanical milling is classified into the two categories of mechanical alloying (MA) and mechanical disordering (MD), depending on different starting materials. MA synthesizes amorphous alloy powders by milling a mixture of elemental crystalline powders, while crystalline alloy or compound powders are directly transformed into the amorphous solid state in MD.

As shown in Fig. 1, MA is a chemical reaction of $mA(crystal)+nB(crystal) \rightarrow A_mB_n(amorphous)$ proceeding from a higher free energy state to a lower one, providing the continuous evolution in the local chemical composition through long-range solid state chemical diffusion. In MD, a phase transformation of $A_mB_n(crystal) \rightarrow A_mB_n(amorphous)$ going from the ground state to an excited state is caused by destroying the long-range

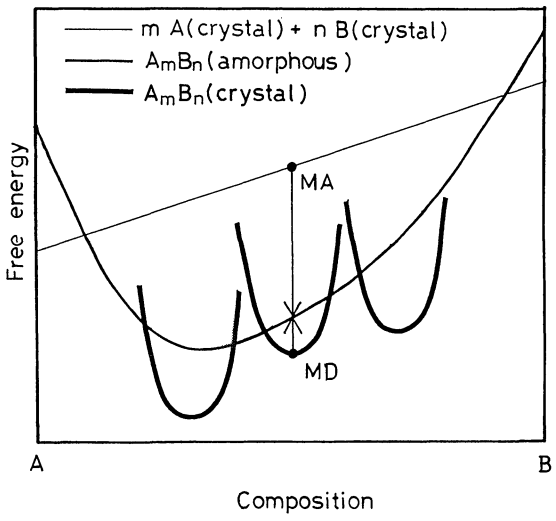

Fig. 1 Schematic free energy of conceivable phases and proceses of mechanical alloying (MA) and mechanical disordering (MD).

periodic structure with relaxing the short-range order without compositional change. Therefore, MA and MD are the reactions going to thermodynamically opposite directions to each other.

This article mentions a new rod milling apparatus developed by us and reviews current achievements on crystal-to-amorphous solid state structure transformation and nonequilibrium nanocrystal formation by mechanical milling.

II. Rod Milling

As mentioned above, mechanical milling is a quite characteristic procedure for forming nonequilibrium solid phases at ambient temperature, compared with conventional processes. However, a difficult problem of mechanical milling has been often pointed out for impurity contamination by milling media during the MA and MD processes. The milling media utilized conventionally are a ball milling apparatus which mainly applies impact force on materials to result in fine powders. Here, the impact force scratches surfaces of the milling media, leading to contamination problems. On the other hand, shear force is more effective for kneading powder mixtures and destroying the long-range periodic structure of crystalline materials to be modified into an amorphous solid structure. The shear force does not deeply contaminate powder specimen with milling media materials during the MA and MD processes, in contrast to the impact force.

In this study, we designed and constructed a new milling apparatus using long rods instead of balls[6], because long rods rotating in a cylindrical vial predominantly supply shear force on materials. In fact, the level of impurity contamination for rod milling can be suppressed below one tenth of that for ball milling. Figure 2 shows a photograph of the rod milling apparatus used in this study, which can control the milling temperature from 100 to 600 K and the milling gas atmosphere from 10^{-3} to 7×10^5 Pa.

Figure 3 shows that the variation of average particle size during MA process of Al-Nb system by using rod milling is obviously classified into three stages as a function of milling time[7]; agglomeration, disintegration and homogenization. In the first stage for agglomeration elemental Al and Nb powders are mechanically joined into a large size particle which often reaches 1 mm in a diameter. The second stage for disintegration is the process for solid state amorphizing transformation where powders are comminuted to 1 mm in the average diameter. The homogenization is the third stage of rod milling where all powders become uniform in their shape (almost spherical), size(less than 1 mm in diameter) and local chemical composition.

The inner structure of a large powder obtained at the end of agglomeration stage, as shown in Fig. 4(a), has a multi-layer structure with a fairly regular interval of several μm, suggesting a significant contribution of shear force during MA process. The short-range structure of amorphous alloy powders obtained at the final stage of homogenization is rather close to that of melt-quenched amorphous alloys in many metal-metal binary systems.

In MD, the agglomeration stage can not be found during the whole process of rod milling, but the average particle size monotonically decreases and crystal-to-amorphous solid state structure transformation proceeds continually with increasing milling time. The homogenization is well developed in the final stage of MD using rod milling.

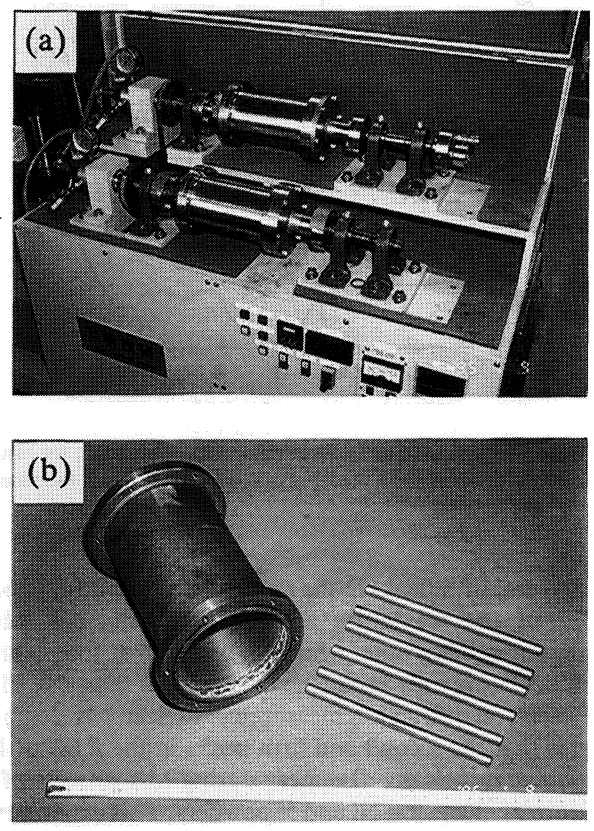

Fig. 2 Photographs of rod milling. (a) the total system and (b) the rod and cylindrical vial.

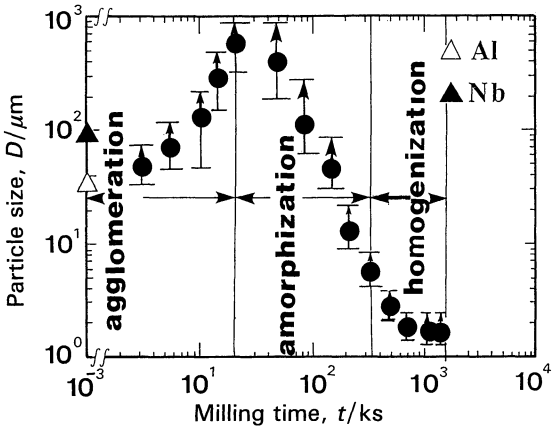

Fig. 3 Variation of the average particle size of $Al_{50}Nb_{50}$ powders as a function of milling time.

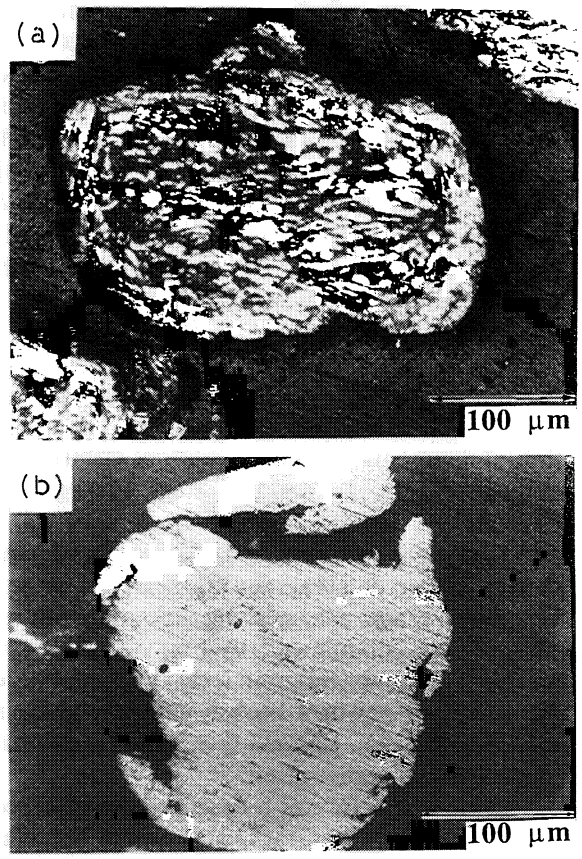

Fig. 4 Optical micrographs of polished $Al_{50}Nb_{50}$ powder particles. (a) after 22 ks and (b) 173 ks of MA time.

III. Crystal-to-Amorphous Solid State Structure Transformation

The first approximation for the topological atomic structure of amorphous metals is described in terms of the dense random packing of hard spheres[8]. However, a dense random packing of soft spheres is better fitted to the realistic structure of amorphous metals, because atoms are rather soft in the metallic state. According to the computer simulation for amorphous metals done by Finney and Wallace[9], polyhedral structure units constructing a dense random packing of soft spheres are almost tetrahedra. The polyhedral structure units found in a closest-packed crystalline structure such as fcc and hcp lattice are exclusively the tetrahedron and octahedron, which exist in an exact ratio of two-to-one. The bcc lattice includes also both the tetrahedral and octahedral structure units, which are distorted but exist still in the ratio of two-to-one. Therefore, the octahedral structure units have to be transformed into the tetrahedral structure units during mechanical milling, if amorphous alloys are directly synthesized from fcc or bcc lattices without formation of intermediate crystalline phases.

Figure 5 is an illustration of the fcc lattice, in which the second and fifth neighboring atoms surrounding a central atom just occupy the key sites so constructing the octahedral structure unit. Therefore, it is expected that the

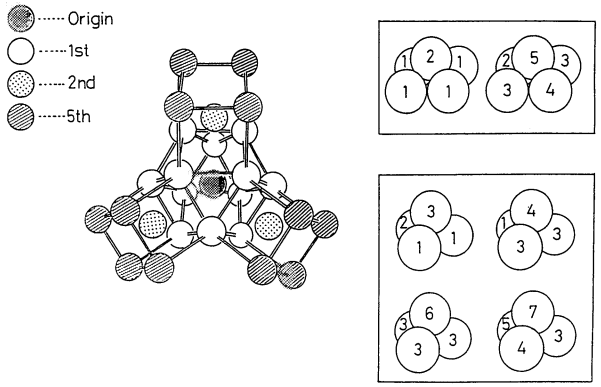

Fig. 5 Atomic arrangement surrounding a central atom in fcc lattice.

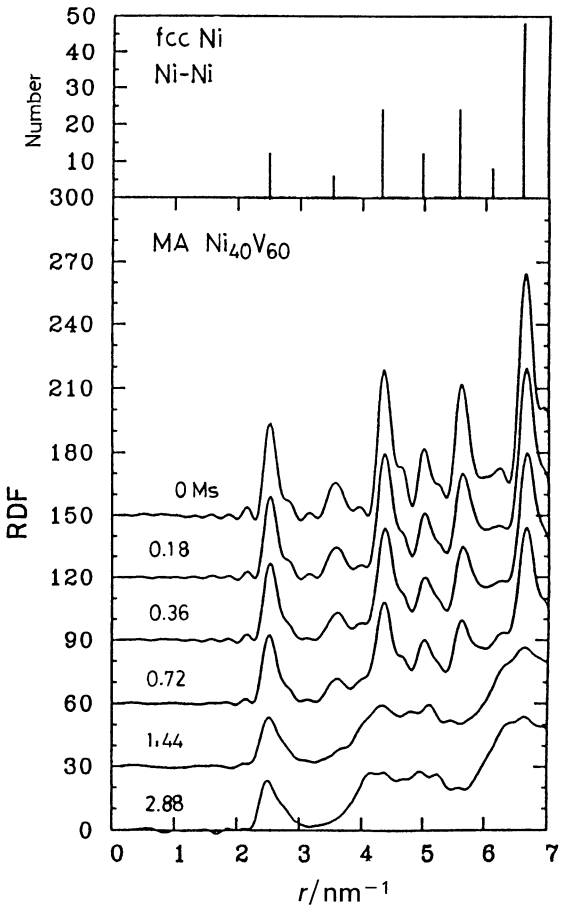

Fig. 6 Neutron total radial distribution functions, RDF, for MA process of 4Ni(fcc)+6V(bcc)→Ni_4V_6(amorphous) as a function of milling time.

second and fifth peaks in the radial distribution function, *RDF*, of the fcc lattice are predominantly lost with increasing milling time, while the first, third, fourth and sixth peaks are only broadened. In fact, as shown in Fig. 6[10], neutron diffraction measurement selectively demonstrates that the second and fifth peaks in the *RDF* of Ni fcc lattice drastically disappear during MA process of a mixture of elemental Ni and V powders. This experiment successfully utilizes the advantage of neutron diffraction that the coherent scattering cross section of V nucleus for

thermal neutrons is negligibly small compared with that of Ni nucleus. Therefore, it is certainly concluded that the topological mechanism of crystal-to-amorphous solid state structure transformation driven by mechanical milling is based on the transition of octahedral structure units into tetrahedral structure units.

The next interesting problem is to examine how the mutual connection between tetrahedral structure units are modified during crystal-to-amorphous solid state structure transformation. An easiest way to do this is to characterize the evolution in the medium-range structure of a crystalline compound consisting of only tetrahedral structure units as a function of milling time[11][12].

As is well known, Ni_4V_6 intermetallic is assigned as the crystalline σ phase ($P4_{2/mnm}$) which includes only tetrahedral structure units as in the Franck-Kasper phases[13]. The Ni–Ni atomic distance in a tetrahedral structure unit is about 0.25 nm. There are three possible ways for connecting tetrahedral structure units to each other; vertex-sharing, edge-sharing and face-sharing, as shown in Fig. 7. The Ni–Ni atomic distance in intertetrahedral structure units is about 0.5 nm for vertex-sharing and 0.4 nm for face-sharing, respectively. The Ni–Ni atomic distance of intermediate length from 0.4 to 0.5 nm is partly caused by edge-sharing between tetrahedral structure units.

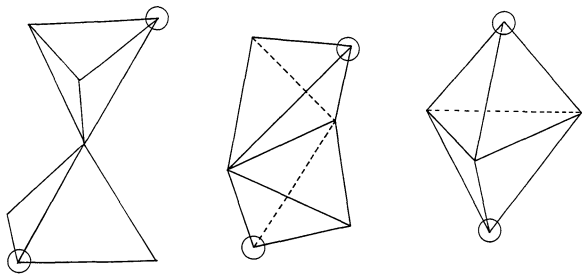

(a) vertex-sharing (b) edge-sharing (c) face-sharing

Fig. 7 Three possible ways of connecting tetrahedral structure units.

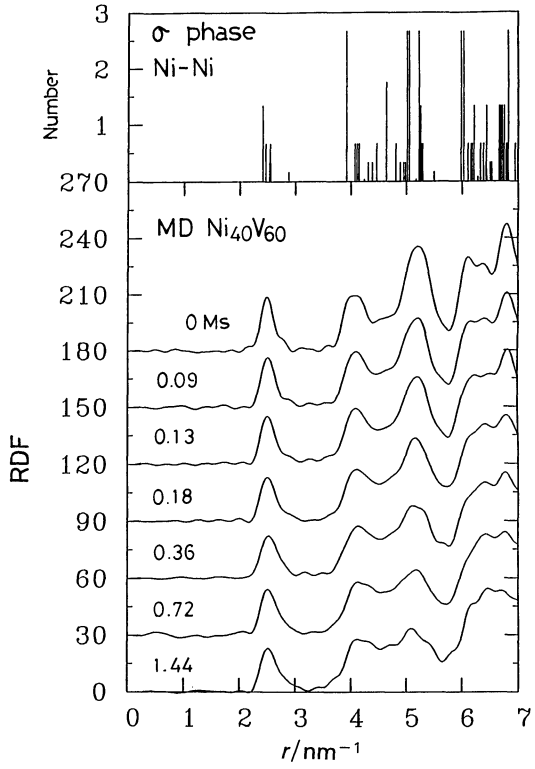

Fig. 8 Neutron total radial distribution functions, RDF, for MD process of Ni_4V_6(crystalline σ phase)→Ni_4V_6(amorphous) as a function of milling time.

Figure 8 shows RDF, for MD process of Ni_4V_6(crystalline)→Ni_4V_6(amorphous) as a function of milling time. In this figure, a peak located around 0.4 nm in the neutron radial distribution function does not vary with increasing milling time, but a peak appearing around 0.5 nm is drastically reduced and an intensity of the radial range from 0.4 to 0.5 nm increases. This implies that edge-sharing between tetrahedral structure units in Ni_4V_6 crystalline σ phase is predominantly destroyed to change into face-sharing and/or edge-sharing between tetrahedral structure units in the Ni_4V_6 amorphous alloy during MD process. The evolution in the medium-range structure during crystal-to-amorphous solid state structure transformation can be understood in terms of the conversion from vertex-sharing to face and/or edge-sharing between tetrahedral structure units.

IV. Thermally Assisted Solid State Amorphization

A mixture of elemental Ta and Al powders is transformed to an amorphous alloy over a wide composition range from 10 to 90 at%Al by MA process at room temperature. El-Eskandarany *et al.* observed that a large particle prepared in the agglomeration stage of MA has a multi-layer structure consisting of bcc Ta(Al) solid solution including excess Al and small amount of fcc Al[14].

This multi-layer structure is transformed into an amorphous solid structure only by heating. As shown in the DTA trace in Fig. 9, the crystal-to-amorphous solid state structure transformation is an exothermic reaction which sharply occur at about 600 K. We call this exothermic solid state reaction "Thermally Assisted Solid State Amorphization (TASSA)". At the moment it is too early to conclude whether the TASSA is driven by asymmetric solid state chemical diffusion between bcc Ta(Al) solid solution and fcc Al or by spontaneous amorphization from bcc Ta(Al) solid solution existing in a higher free energy state.

Such an unstable crystalline solid solution is formed for Zr–Al and Nb–Al systems, too[7][15]. The low-energy milling using rod milling apparatus may play an essential role for formation of this kind of unstable crystalline phases having multi-layer structure. Figure 4(b) shows that multi-layer structure completely disappears after finishing TASSA. Since utilization of TASSA reduces substantially the milling time for reaching the amorphous solid state, the difficult problem of impurity contamination during mechanical milling can be almost avoided.

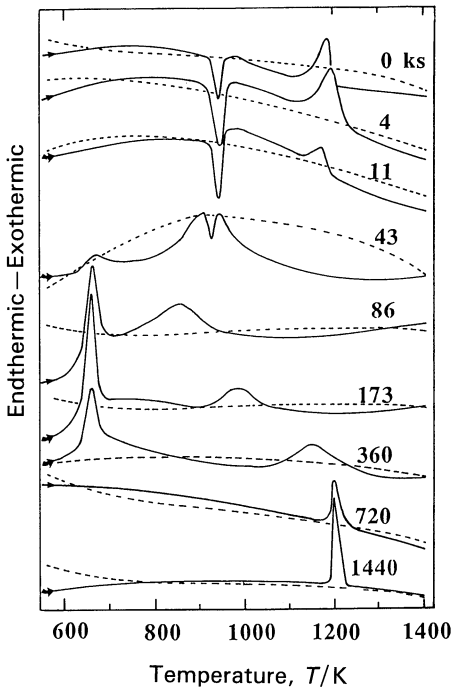

Fig. 9 DTA curves (solid lines) for $Al_{50}Ta_{50}$ alloy powder as a function of MA time. Dashed lines indicate second heating runs.

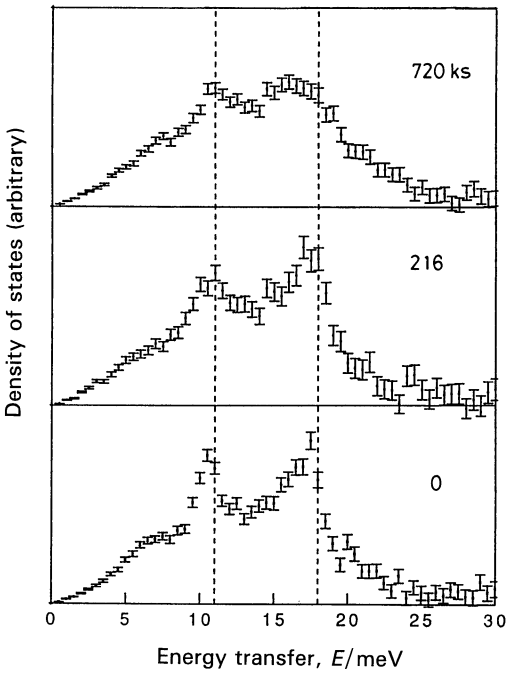

Fig. 10 Atomic vibrational energy spectra of Ta metal powders measured at room temperature by inelastic neutron scattering as a function of rod milling time.

V. Comminution to Nanocrystalline Ta Metal Powders

When Ta metal powders are comminuted by rod milling in argon gas atmosphere at room temperature, the refinement of crystalline size and the accumulation of atomic level strain drastically occur in an initial stage of milling and then are saturated at a certain milling time of about 720 ks[16]. The final crystalline size is about 10 nm in average diameter and the stored strain reaches about 1.3×10^{-2}. However, the structural transformation from crystal to amorphous solid is found, if Ta metal is contaminated by Fe atoms coming from the milling media beyond a critical limit of about 2 at%Fe.

Figure 10 shows the evolution in the energy spectrum of atomic vibration of Ta metal during rod milling, which were measured at room temperature by inelastic neutron scattering. The profile of the vibrational spectrum shows little change in the low energy range below 10 meV after 720 ks milling. This observation obviously contrasts against a conventional explanation that the phonon softening should happen in nanocrystalline metals containing liquid-like grain boundaries and excess lattice defects. We have also found that the low-temperature specific-heat of Ta metal powders milled for 720 ks is not significantly different from that before milling.

The atomic vibrational modes around 11 and 18 meV are dramatically damped with increasing milling time, as shown in Fig. 10. The atomic vibrational mode of 11 meV corresponds to the longitudinal acoustic phonon in [111] direction and the transverse acoustic phonon in [111] direction in (110) plane in bcc Ta crystal, while the atomic vibrational mode of 18 meV comes from the longitudinal acoustic phonon in [111] and [100] directions and the transverse acoustic phonon in [110] direction[17]. The bcc crystal is well known to have the slip plane of (110) and the slip direction of [111][18]. Therefore, we can straightly conclude that bcc Ta metal powders are comminuted to nanocrystalline grains by the glide of dislocations induced by the shear force supplied by rod milling.

We found unexpectedly a large intensity in the vibrational spectrum of Ta metal powders milled for 720 ks over a high-energy range from 50 to 200 meV. This intensity is predominantly contributed from the high energy vibration of hydrogen atoms included in Ta metal powders during rod milling. How hydrogen atoms come in Ta metal during rod milling is not clear at the moment. However, it is noteworthy that the mechanical comminution of metals having high hydrogen absorbing capacity may be often influenced by the contamination due to hydrogen atoms.

VI. Formation of Ternary Metal-Metal-Metalloid Amorphous Alloys

Ni–P and Cu–P are the most classical systems in the investigation of amorphous alloys, becauce they have been produced by electroplating, liquid quenching, vapor quenching, etc.[8] For industrial application such as catalysis, ternary alloys are more useful and $Cu_{71}Ni_{11}P_{18}$ is a typical example. By mechanical milling, amorphous phases are completely formed in ternary $Cu_{71}Ni_{11}P_{18}$ and $Cu_3P + 11\%Ni$ powders[19][20], but partially formed in $Cu_{80}P_{20}$ and $Ni_{82}P_{18}$ powders, in contrast to no formation in $Cu_{87}Ni_{13}$ and Cu_3P[21]. A careful check of their milling process by X-ray diffraction indicates that the following amorphization process in mechanically milled

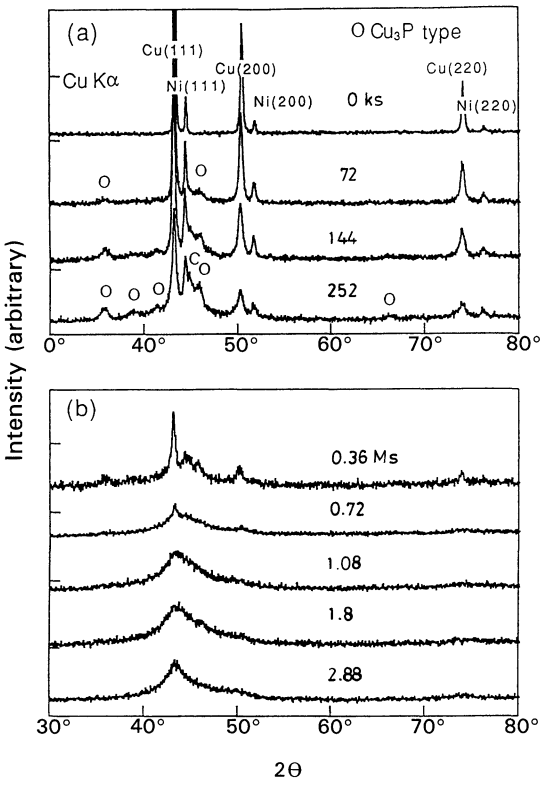

Fig. 11 X-ray diffraction patterns of mechanically milled $Cu_{71}Ni_{11}P_{18}$ alloy powders for different milling times. (a) at the early stage and (b) at the final stage.

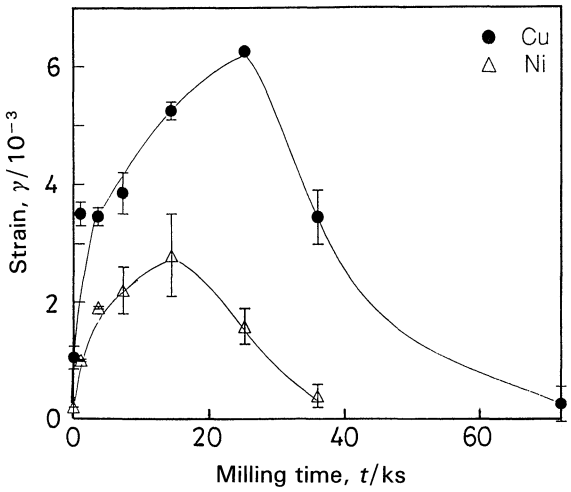

Fig. 12 Root mean square strain for different phases as a function of milling time for mechanically milled $Cu_{71}Ni_{11}P_{18}$ alloy powders.

$Cu_{71}Ni_{11}P_{18}$ alloy powders (see Fig. 11). At the initial stage of milling, elemental Cu, Ni and P particles are comminuted into smaller ones and interdiffusion is much enhanced between small elemental particles with increasing milling time. In the middle stage, Cu_3P intermetallic is first formed, indicating the preferential reaction between Cu and P in spite of the random mixing of Cu, Ni and P. No formation of Ni_3P is probably due to its higher activation energy of reaction than that of Cu_3P. In the final stage, an amorphous phase is formed by the reaction of the Cu_3P intermetallic and Ni phases, where the amorphous phase is rather heterogeneous. With further increasing milling time, the amorphous phase becomes homogeneous. These aspects have been confirmed by differential scanning calorimetry (DSC) and electron microscopy measurements[19]-[21].

Since both mechanical milling and rapid quenching are massproduction process of amorphous alloys, it is worthwhile to mention an advantage of mechanical milling. The DSC traces reveal a broad but single exothermic peak for the $Cu_{71}Ni_{11}P_{18}$ amorphous alloy powders produced by mechanical milling, while they reveal several exothermic peaks in liquid-quenched $Cu_{71}Ni_{11}P_{18}$ amorphous alloy ribbons[20]. These results demonstrate that the amorphous alloys obtained by low-energy mechanical milling are more homogeneous than those obtained by liquid quenching,

A root mean square strain stored during milling process has been estimated from the integral widths of X-ray diffraction peaks[22]. As shown in Fig. 12, the stored strain increases in the initial stage, while it decreases in the middle and final states, being accompanied with formation of the amorphous phase and refinement of the crystallite sizes. Therefore, the amorphous phase formation is ascribable to the release of stored strain energy. Of course, the amorphous phase formation by mechanical milling is also attributed to the free energy gain of ternary mixture with a higher entropy, because no complete amorphous phase formation has been realized in the binary alloys.

VII. Formation of Nonequilibrium bcc and Amorphous Ni Metals

In the equilibrium phase diagram, there is B2 type NiAl intermetallic, which is basically bcc[23]. Although a disordered bcc phase has been hardly obtained by rapid quenching, we can obtain almost disordered bcc Ni-Al alloys by high energy ball milling and amorphous Ni-Al alloys at Al-rich off-stoichiometric composition by low energy ball milling[24][25]. Since Al is dissolved in alkaline solution, more than 95%Al can be removed from Ni-Al powders by leaching in KOH solution. Since the topotactic leaching process occurs very slowly, the X-ray diffraction patterns reveal no considerable change in the original bcc and amorphous structures, as shown in Fig. 13. These phenomena clearly demonstrate that the addition of chemical process to mechanical milling is very useful to produce nonequilibrium metallic phases, because mechanically milled powders are very reactive due to a large amount of strain and defects and their small particle sizes.

At low temperatures, bcc and amorphous Ni powders exhibit paramagnetic characters[24][25]. Figure 14 shows the temperature dependence of magnetization, σ_S, for bcc and amorphous Ni. Since contamination of ferromagnetic impurity and retaining of original fcc Ni powders are rather serious in the specimens made through

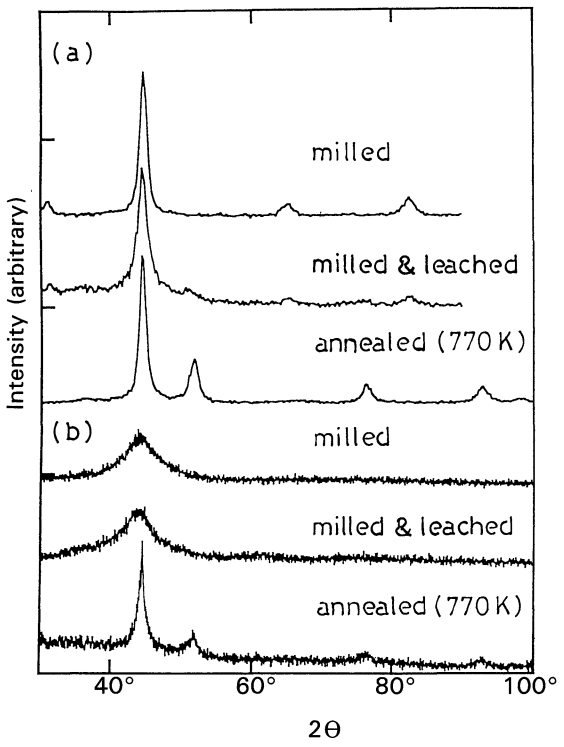

Fig. 13 X-ray diffraction patterns of mechanically-milled and leached Ni–Al alloy powders. (a) $Ni_{35}Al_{65}$ specimens made by high energy ball milling and (b) $Ni_{40}Al_{60}$ made by low energy ball milling.

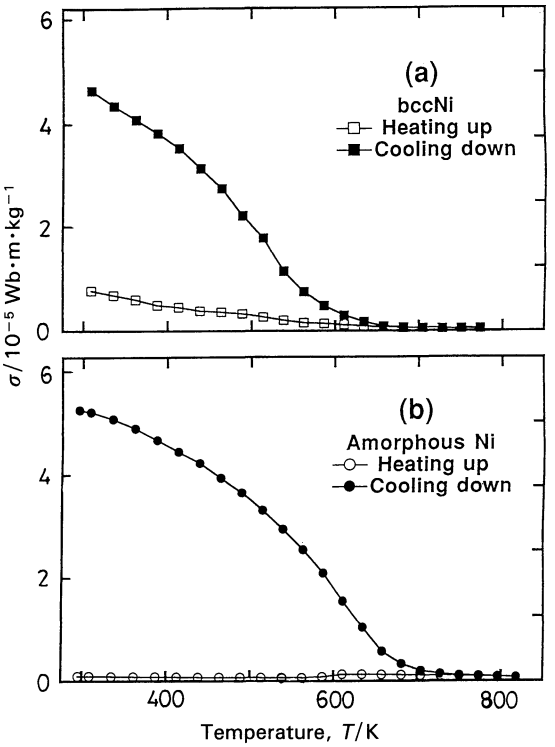

Fig. 14 Thermomagnetic curves of mechanically-milled and leached Ni–Al alloy powders. (a) $Ni_{35}Al_{65}$ specimens made by high energy ball milling and (b) $Ni_{40}Al_{60}$ made by low energy ball milling.

the high energy milling process, σ_S, is rather large of 6.3×10^{-6} Wb m/kg at 300 K. However, σ_S is neglegibly small in the specimens made through the low energy milling process. Since the DSC traces of bcc and amorphous Ni specimens reveal broad exothermic peaks above 450 K, indicating the phase transformation to the fcc phase, σ_S is finite above 500 K and it decreases up to the Curie temperature of the ferromagnetic fcc phase. The paramagnetism of bcc and amorphous Ni has been theoretically predicted by the band structure calculations[26]. The low temperature specific heat measurements indicate that the values of the electronic specific heat coefficient, γ, are twice larger than those of fcc Ni and the annealed specimens[27]. This is owing to the higher density of states at the Fermi level for paramagnetic bcc and amorphous Ni phases and the contribution of paramagnon in comparison with that of fcc Ni.

VIII. Formation of Nonequilibrium Crystalline Alloys

1. fcc Ce–Yb alloys

Although Ce and Yb are immiscible in the equilibrium crystalline state[23], Ce–Yb fcc solid solutions can be obtained by mechanical milling[28]. DSC trace reveals a broad exothemic peak at about 500 K, suggesting the phase separation to the equilibrium fcc Ce and Yb phases. The magnetic susceptibility increases with increasing Yb concentration and almost follows the Curie-Weiss law for $T>40$ K. Figure 15 shows the effective Bohr magneton, μ_{eff}, of the present fcc Ce–Yb alloys estimated from the Curie-Weiss constant. The values of μ_{eff} markedly deviate upward from the straight line connecting between the μ_{eff} values of Ce^{+3} and Yb^{+2}, but smaller than the line connecting the values of Ce^{+3} and Yb^{+3}[29], indicating that the Yb atoms are in mixed valent states, because the total angular momentum, $J=0$ ($\mu_{eff}=0\mu_B$) for the divalent state and $J=7/2$ ($\mu_{eff}=4.5\mu_B$) for the trivalent state.

Within Miedema's semi-empirical model[30], the heat of formation, ΔH, of the binary Ce–Yb alloys is positive in the whole concentration range predicting no intermetallic

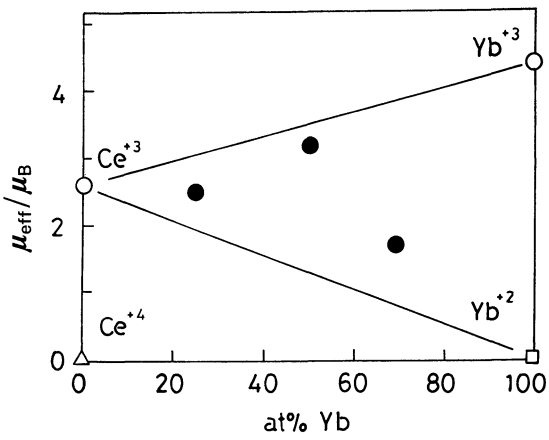

Fig. 15 The effective magnetic moment, μ_{eff}, for the fcc Ce–Yb alloy powders produced by mechanical milling.

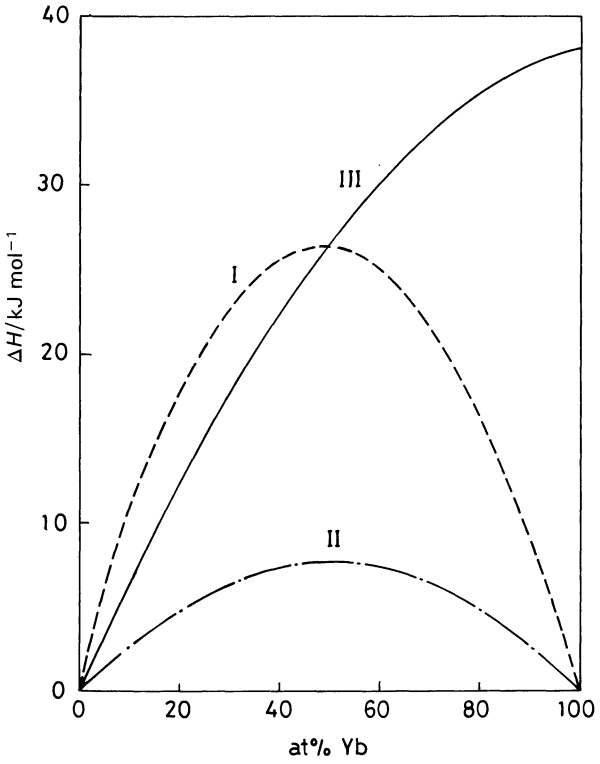

Fig. 16 The heat of formation, ΔH, for the Ce-Yb alloy system. The curve A: trivalent Yb, the curve B: divalent Yb and the curve C: trivalent Yb by correcting for the transformation energy of Yb^{+2} to Yb^{+3}.

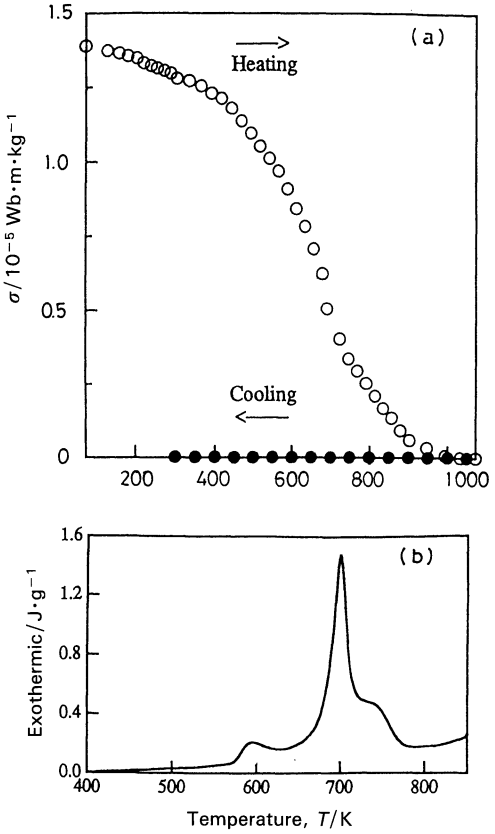

Fig. 17 (a) Thermomagnetic curves and (b) DSC trace for $Mn_{30}Al_{70}$ alloy powder.

compound (see Fig. 16). For the equiatomic alloy, ΔH of Ce^{+3}-Yb^{+3} system is comparable to 26 kJ/mol for the Ce^{+3}-Yb^{+2} system. In the low temperature specific heat measurements[31], the electronic specific heat coefficient is strongly enhanced as in typical heavy fermion Ce and Yb alloys, suggesting that the 4f electron band is not fully occupied. The 4f electrons are mixed with conduction electrons and they strongly correlate with each other to form a Kondo resonance state at the Fermi level[32]. Moreover, the Kondo coupling of local magnetic moments of Yb atoms with conduction electron spins gives rise to the free energy gain and overcomes the increase of elastic energy with alloying. At the same time, since the lattice contraction enhances the Kondo coupling, they may cooperatively contribute to the formation of the metastable fcc phase.

2. α-Mn type Mn-Al solid solution

In contrast to a very narrow range of the primary α-Mn phase in the equilibrium phase diagram[23], a wide concentration range of the nonequilibrium α-Mn type solid solution was obtained in mechanically milled Mn-Al alloy powders[33], where their significant peaks do not shift from those of the pure α-Mn is detected in their X-ray diffraction patterns. These alloys are ferromagnetic at low temperatures. The spontaneous magnetization, σ_S, increases rapidly during the initial stage of milling owing to the Al solution in the α-Mn phase. At 290 K, σ_S, is largest, about 1.4×10^{-5} Wb m/kg and the coercive force, H_C, is about 12 A/m for Mn-70 at%Al alloy powders mechanically milled for 1.08 Ms. The DSC trace of this alloy reveals broad exothermic peak at 680 K, indicating the phase transformation from the α to γ_2 phases. As shown in Fig. 17, σ_S, gradually decreases with increasing T up to 900 K. After heating the specimens above 1000 K, σ_S, is negligibly small, being consistent with the formation of the nonmagnetic γ_2 phase.

In the Mn-Al alloys quenched from the high temperature ε phase, the metastable τ phase is obtained at around the equiatomic concentration by low temperature annealing[23]. The τ phase is a well-known nonferrous ferromagnet[34]. However, since no significant Bragg peak corresponding to this phase was detected in the X-ray diffraction pattern, the contribution from the τ phase to the ferromagnetism in the mechanically milled Mn-Al alloys can be discarded. The ferromagnetism in mechanically milled α-Mn-Al powders is most simply attributed to partial collapse of antiferromagnetism: a large amount of lattice defects induce unbalance of noncolinearly aligned magnetic moments. Based upon local density functional approximation combined with KKR-CPA[35], moreover, a ferromagentic Mn is contemplated in Mn-trivalent metal alloys: the formation of bonding and antibonding states by Al dilution brings the density of states of the 3d band at the Fermi level in Mn close to that in ferromagnetic Fe. In order to understand the origin of the ferromagnetism in the nonequilibrium α-Mn-type Mn-Al alloys, measurements of microscopic atom displacement

and the magnetic hyperfine field are desired.

IX. Concluding Remarks

For both the comminution to nanograin size and the crystal-to-amorphous solid state structure transformation which are driven by mechanical milling, shear force works more effectively than impact force. Rod milling is a successful method for employing shear force. Moreover, formation of nonequilibrium crystalline and amorphous phases by contamination of oxygen and impurities from milling media has been plausible even in an immiscible binary system, if the positive enthalpy is compensated by negative enthalpy of oxides and solid solutions with impurities. Since the rod milling can avoid serious impurity contamination during mechanical milling, it is highly recommended.

The simple destruction of the long-range order in a crystalline lattice does not result in the solid state amorphization. Broadening of the Bragg reflection peaks in the crystalline state is rapidly saturated at an early stage of mechanical milling. The topological rearrangement in the short- and medium-range structure by accumulating defects and excess energies has to take place in the crystal-to-amorphous solid state structure transformation during the milling process. The topological mechanism of solid state transformation from crystalline to amorphous solid by mechanical milling can be understood in terms of the mutation of octahedral structure units into tetrahedral structure units, and reconnection of tetrahedral structure units from vertex-sharing to face and/or edge sharing. Even though the mechanical milling is a stochastic and heterogeneous process, a certain long time millng shapes a macroscopically heterogeneous mixture into an atomically homogeneous one.

As discussed above, kneading and atomic level contact of elemental powder mixtures increase their mixing entropy, being favorable for formation of nonequilibrium disordered crystalline phases. Moreover, several crystalline phases different from the equilibrium one may be optimized in mechanically milled systems, because accumulation of strain and defects influences the electronic state of valence electrons, and provides other thermodynamical freedoms. In this context, we should challenge to explore conceivable crystalline alloy phases which have electronic and magnetic characteristics different from those of the equilibrium phase.

So far several models for the thermodynamic mechanism of mechanically driven nanocrystal formation and solid state amorphization have been proposed: local melt-quenching[36], asymmetric solid state interdiffusion[37], excess defect accumulation[38], lowering of the meting point[39] and phase separation in supersaturated solid solution[40], elasticity instability[41] and so on. However, the structural mechanism studied in this work has been little reported. In particular, there is need to focus on the role of low-energy medium-range collective excitation in the crystal-to-amorphous solid state structure transformation by measurement of neutron dynamical structure factors. In order to make the mechanical milling as a unique process for materials synthesis, fundamental investigations relating atomic-scale structure to thermodynamics and kinetics must be emphasized.

Acknowledgments

The studies described in this article have been performed by the collaboration with Dr. K. Aoki, Dr. M. S. El-Eskandarany, Dr. T. Fukunaga, Dr. T. Hihara, Dr. Y. Homma, Dr. E. Ivanov, Dr. K.-J. Kim, Dr. S. A. Makhlouf, Mr. M. Murakami, Dr. K. Shibata, Dr. H. Yamauchi and Mr. K. Yanai. The authors wish to thank Dr. K. Takada for ICP analysis, and Mr. S. Ono and Mr. K. Wakoh for their experimental support. This work was partially supported by a Grant-in-Aid for Scientific Researches (Grant No. 03555139, No. 03452029 and 06452323) given by the Ministry of Education, Science and Culture, Japan.

REFERENCES

(1) *Proc. Conf. on Solid State Amorphizing Transformations* (Los Alamos, U.S.A., 1987), ed. by R. B. Schwarz and W. L. Johnson, in J. Less-Common Metals, **140** (1988).
(2) *Proc. Int. Symp. on Mechanical Alloying* (Kyoto, Japan, 1991) in Materials Science Forum, **88/90** (1992) ed. by P. H. Shingu and references therein.
(3) *Proc. European Workshop on Ordering and Disordering in Alloys* (Grenoble, France, 1991), ed. by A. R. Yavari, Elsevier Applied Science, London and New York, (1992) and references therein.
(4) *Proc. Int. Symp. on Non-Equilibrium Solid Phases of Metals and Alloys* (Kyoto, Japan, 1988), ed. Y. Nakamura and H. Fujimori in Trans. JIM, 29 Supplement (1988) and references therein.
(5) *Special Issue on Solid State Amorphizing Transformations*, ed. by D. E. Luzzi in J. Alloys and Compounds, **194** (1993) No. 2.
(6) M. S. El-Eskandarany, K. Aoki and K. Suzuki: J. Less-Common Metals, **167** (1990), 113.
(7) M. S. El-Eskandarany, K. Aoki and K. Suzuki: Metall. Trans., **23A** (1992), 2131.
(8) T. Masumoto, K. Suzuki, H. Fujimori and K. Hashimoto: *Materials Science of Amorphous Metals*, Ohm-sha, Tokyo, (1982).
(9) J. L. Finney and J. Wallace: J. Non-Cryst. Solids, **43** (1981), 165.
(10) T. Fukunaga, Y. Homma, M. Misawa and K. Suzuki: J. Non-Cryst. Solids, **117/118** (1990), 721.
(11) K. Suzuki: J. Phys.: Condens. Matter, **3** (1991), F39.
(12) K. Suzuki and T. Fukunaga: J. Alloys and Compounds, **194** (1993), 303.
(13) W. B. Pearson: *A Handbook of Lattice Spacings and Structures of Metals and Alloys*, Pergamon, Oxford, (1958).
(14) M. S. El-Eskandarany, K. Aoki and K. Suzuki: J. Non-Cryst. Solids, **150** (1992), 472.
(15) M. S. El-Eskandarany, K. Aoki and K. Suzuki: J. Appl. Phys., **71** (1992), 2924.
(16) M. Murakami: Master Thesis (Tohoku University, 1993).
(17) A. Magerl, N. Stump, W. D. Teuchert, V. Wagner and G. Alfeld: J. Phys.: Solid State Phys., **10** (1977), 2783.
(18) E. N. da C. Andrade: Proc. Phys. Soc., **52** (1940), 1.
(19) K. J. Kim, M. S. El-Eskandarany, K. Sumiyama and K. Suzuki: J. Non-Cryst. Solids, **155** (1993), 165.
(20) K. J. Kim, K. Sumiyama and K. Suzuki: submitted to J. Alloys and Compounds.
(21) K. J. Kim, K. Sumiyama and K. Suzuki: J. Non-Cryst. Solids, **168** (1993), 232.
(22) G. K. Williamson and W. H. Hall: Acta Metall., **1** (1953), 22.
(23) T. B. Massalski, H. Okamoto, P. R. Subramanian and L. Kacprazak: *Binary Alloy Phase Diagrams 2nd Ed*, ASM International, Ohio, (1990).
(24) E. Ivanov, S. A. Makhlouf, K. Sumiyama, H. Yamauchi, K.

Suzuki and G. Golubkuva: J. Alloys and Compounds, **185** (1992), 25.
(25) S. A. Makhlouf, K. Sumiyama and K. Suzuki: J. Alloys and Compounds, **199** (1992), 119.
(26) V. L. Moruzzi, P. M. Marcus, K. Schwarz and P. Mohn: Phys. Rev., **B34** (1986), 1784.
(27) S. A. Makhlouf, K. Sumiyama, E. Ivanov, H. Yamauchi, T. Hihara and K. Suzuki: Mat. Sci. Eng., **A181/A182** (1994), 1184.
(28) E. Ivanov, K. Sumiyama, H. Yamauchi, K. Yanai and K. Suzuki: J. Alloys and Compounds, **198** (1993), 105.
(29) J. Jensen and A. R. Mackintosh: *Rare Earth Magnetism—Structures and Excitations—*, Oxford Science Publications, (1991).
(30) A. R. Miedema and A. K. Niessen: Physica, **114B** (1982), 367.
(31) K. Sumiyama, K. Yanai, H. Yamauchi, E. Ivanov and K. Suzuki: Mat. Sci. Eng., **A181/A182** (1994), 1268.
(32) N. B. Brandt and V. V. Moshchalkov: Adv. Phys., **33** (1984), 373.
(33) K. J. Kim, K. Sumiyama and K. Suzuki: J. Alloys and Compounds, (1994) in press.
(34) H. Kono: private communication.
(35) H. Akai: to be published in Phys. Rev. B.
(36) A. Y. Yermakov, Y. Y. Yurchikov and V. A. Barinov: Phys. Met. Metallogr., **52** (1981), 50.
(37) R. B. Schwarz, R. R. Petrich and C. K. Saw: J. Non-Cryst. Solids, **76** (1985), 281.
(38) C. C. Koch, O. B. Cavin, C. G. McKamey and J. O. Scarborough: Appl. Phys. Lett., **43** (1983), 1017.
(39) H. J. Fecht, G. Han, Z. Fu and W. L. Johnson: J. Appl. Phys., **67** (1990), 1744.
(40) W. Biegel, W. Schaper, H.-U. Krebs, J. Hoffmann, H. C. Freyhardt, R. Bush and R. Bormann: Coll. Phys., **C4** (1990), C4-189.
(41) W. L. Johnson: Prog. Mater. Sci., **30** (1986), 81.